NANO LETTERS

Letter

pubs.acs.org/NanoLett

Exploring a Proximity-Coupled Co Chain on Pb(110) as a Possible Majorana Platform

Michael Ruby,[†] Benjamin W. Heinrich,[*,†] Yang Peng,[†,‡] Felix von Oppen,[†,‡] and Katharina J. Franke[†]

[†]Fachbereich Physik, [‡]Dahlem Center for Complex Quantum Systems, Freie Universität Berlin, 14195 Berlin, Germany

Supporting Information

ABSTRACT: Linear chains of magnetic atoms proximity coupled to an *s*-wave superconductor are predicted to host Majorana zero modes at the chain ends in the presence of strong spin−orbit coupling. Specifically, iron (Fe) chains on Pb(110) have been explored as a possible system to exhibit topological superconductivity and host Majorana zero modes [Nadj-Perge, S. et al., *Science* **2014**, *346*, 602−607]. Here, we study chains of the transition metal cobalt (Co) on Pb(110) and check for topological signatures. Using spin-polarized scanning tunneling spectroscopy, we resolve ferromagnetic order in the *d* bands of the chains. Interestingly, also the subgap Yu−Shiba−Rusinov (YSR) bands carry a spin polarization as was predicted decades ago. Superconducting tips allow us to resolve further details of the YSR bands and in particular resonances at zero energy. We map the spatial distribution of the zero-energy signal and find it delocalized along the chain. Hence, despite the ferromagnetic coupling within the chains and the strong spin-orbit coupling in the superconductor, we do not find clear evidence of Majorana modes. Simple tight-binding calculations suggest that the spin−orbit−split bands may cross the Fermi level four times which suppresses the zero-energy modes.

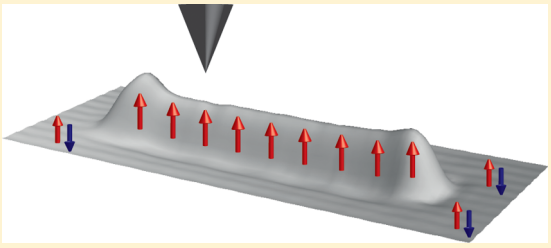

KEYWORDS: *Yu−Shiba−Rusinov state, spin polarization, topological superconductivity, Majorana fermion, proximity-coupled chain*

Low-dimensional structures proximity coupled to an *s*-wave superconductor can support topologically protected Majorana zero modes, which obey non-Abelian statistics and are potentially useful for fault-tolerant quantum computation.[1−3] Although realizing a topological superconductor is challenging, there are promising results for various experimental platforms.[4−8] The simplest systems emulate a model first proposed by Kitaev:[9] a tight-binding chain for a spinless *p*-wave superconductor in one dimension. This system with nearest-neighbor hopping and pairing carries zero energy excitations at the chain ends which are protected when an odd number of bands cross the Fermi level. Ferromagnetic chains of atoms adsorbed on an *s*-wave superconductor in the presence of strong spin−orbit coupling have been suggested as an intriguingly simple experimental realization.[10] By proximity coupling Cooper pairs enter the chain, which induces *p*-wave superconductivity in the chain and turns it into a topological superconductor. The occurrence of Majorana modes has been predicted to be near universal in sufficiently long chains of transition-metal atoms on Pb.[10] Such systems fulfill the requirements for a topological superconducting phase: a large exchange splitting of the *d* bands, strong Rashba spin−orbit coupling originating from the superconducting substrate, and proximity induced superconductivity. In addition, topological superconductivity requires an odd number of Fermi points in half of the Brillouin zone of the one-dimensional chain.

Nadj-Perge et al. have presented indications of Majorana zero modes in iron (Fe) chains on Pb(110).[5] Additional experiments have stimulated further discussions.[11−13] The appealing simplicity of this platform motivates us to explore chains of another 3*d* element. We replace iron by cobalt (Co), thereby keeping the one-dimensional band structure of the chain similar while modifying the number of *d* electrons and hence the band filling.

The experiments are performed in a SPECS JT-STM at a temperature of 1.1 K under UHV conditions. The Pb(110) single crystal (T_c = 7.2 K) is cleaned by cycles of sputtering and annealing until atomically flat and clean terraces are observed. Co chains were prepared by e-beam evaporation from a cobalt rod (99.995% purity) onto the clean surface. We use cobalt-covered W-tips for spin-polarized measurements and check their spin sensitivity prior to the measurement on bilayer cobalt islands on Cu(111). These nanoislands possess an out-of-plane magnetization and represent a standard reference system.[14] The hysteresis loop in an out-of-plane magnetic field reveals a sizable tip remanence at zero field and a coercivity of ≈50 mT [see the Supporting Information (SI)]. Pb-covered, superconducting tips[15] are used to provide an energy resolution of ≃60 μeV, well beyond the Fermi−Dirac limit. The differential conductance dI/dV as a function of sample bias was recorded using standard lock-in technique at 912 Hz with a bias modulation of V_{mod} = 15 μV_{rms} (Pb tip, ± 4 mV), 50 μV_{rms} (Co tip, ± 4 mV), 5 mV_{rms} (±0.3 V), and 10 mV_{rms} (±1.5 V), respectively.

Received: April 24, 2017
Revised: June 21, 2017

DOI: 10.1021/acs.nanolett.7b01728
Nano Lett. XXXX, XXX, XXX−XXX

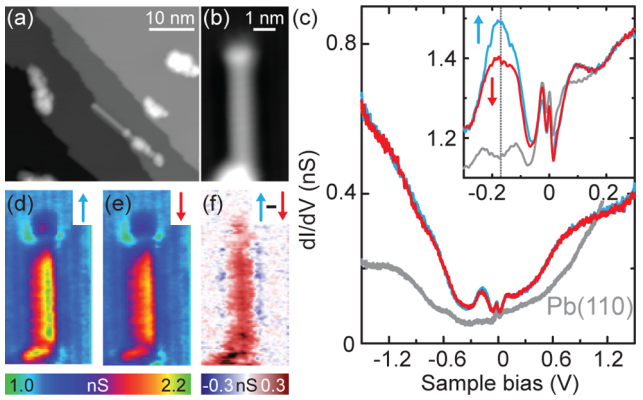

Figure 1. Co chain on Pb(110). (a) After deposition on Pb(110), Co forms clusters and 1D chains. Set point: 100 mV, 50 pA. (b) Close-up of a 1D Co chain of length ≈5.5 nm. Set point: 500 mV, 50 pA. (c) Spin-polarized dI/dV spectra of the chain shown in panel b (blue, red) and of pristine Pb(110) (gray). The blue (red) curve is acquired in a +(−)0.3 T magnetic field along the surface normal. The field reversal ensures opposite tip magnetization (in the following ↑ and ↓). Set point: 1.5 V, 400 pA. The inset shows spectra in a narrower energy window. Set point: 300 mV, 400 pA. Panels d and e show dI/dV maps at V = −170 mV in fields of + and −0.3 T, respectively, revealing spin-dependent dI/dV intensities all along the chain. Feedback: 300 mV, 400 pA. (f) Map of the difference signal of panels d and e characterizing the spin polarization of the chain's d band.

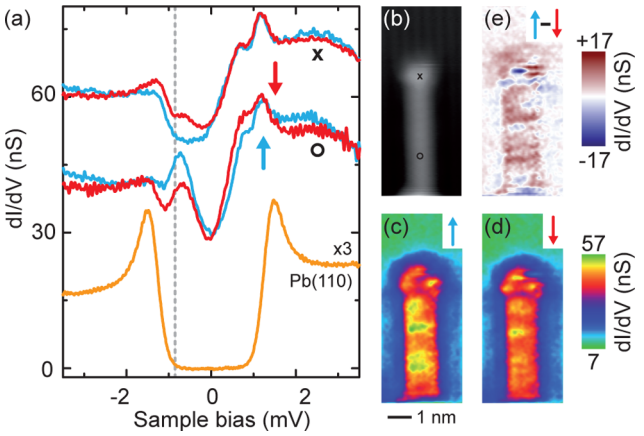

Figure 2. (a) dI/dV spectra taken at the two positions on the Co chain depicted in the topography in panel b. For clarity, the spectrum taken on the bare surface is divided by three. The data are recorded at 0 T with a spin-polarized tip with a remanence which has an out-of-plane component relative to the sample surface. Parallel and antiparallel orientations are indicated by ↑ (blue) and ↓ (red). Set point: 4 mV, 200 pA. The dashed line at −850 μV marks, where the dI/dV maps in panels c and d are recorded with parallel and antiparallel tip-magnetization, respectively. The feedback was opened at 4 meV, 200 pA where no spin polarization is observed. (e) Map of the difference signal of panels c and d characterizing the spin polarization of the YSR bands of the chain.

At a sample temperature of 263 K, Co deposition onto Pb(110) yields clusters and 1D chains with lengths of up to ≃11 nm (Figure 1a). These resemble the Fe chains studied earlier.[5,11−13] In most cases, the chains emerge from a Co cluster and follow the [1$\bar{1}$0] direction of the (110) surface. At the opposite end, the chains are either flat or terminated by a small protrusion as was also observed in the case of Fe. Figure 1b presents a closeup of a typical chain of ≈5.5 nm length (measured between chain end and the onset of the cluster).

To probe the magnetic properties of the chain,[16] we employ Co-coated tips, which have been tested for their out-of-plane spin contrast beforehand (see SI). We resolve a resonance at −0.17 V (Figure 1c), which exhibits different intensities for oppositely polarized tips (labeled ↑ and ↓). We ascribe this resonance to the van Hove singularity of a spin-polarized Co d band (for additional spectra along the same chain, see the SI). The magnetic order of the chain is revealed by dI/dV maps at the energy of the van Hove singularity (Figure 1d,e). The intensity along the chain is stronger for tip$_\uparrow$ than for tip$_\downarrow$. In the difference map shown in Figure 1f, this leads to a positive contrast (red) on the chain. The uniform contrast along the Co chain suggests that it is in a ferromagnetic state, similar to Fe chains on Pb(110), although we cannot exclude a more complex spin arrangement with the out-of-plane spin component being preserved along the chain.

Figure 2 explores magnetic signatures within the superconducting energy gap using the same tip as before. The dI/dV spectrum on pristine Pb(110) shows a BCS-like gap, broadened by the Fermi−Dirac distribution of the tip at 1.1 K (Figure 2a). On the chain, there are broad resonances within the gap, which vary in intensity along the chain (see the SI for additional spectra). These resonances reflect Yu−Shiba−Rusinov[17−19] (YSR) bound states, which result from the exchange coupling between the spin-polarized Co d states and the superconducting substrate. When measured with opposite tip magnetization (which is possible in zero field because of a sizable magnetic remanence of the tip), the spectra are qualitatively similar but differ in signal strength. The overall intensity at negative (positive) energies is stronger (weaker) for tip$_\uparrow$ than for tip$_\downarrow$. This is clearly revealed by the spin contrast map (Figure 2e), which exhibits an overall positive polarization along the chain at −850 μV, but a negative polarization at +850 μV (see the SI). This sizable spin polarization is remarkable because it provides direct experimental evidence for the magnetic nature of YSR bands, which was predicted theoretically decades ago.[17−19] The hybridization of YSR states of neighboring adatoms along the chain results in spin-polarized bands. Although confinement effects and potential variations cause intensity variations of the YSR bands,[12] the spin polarization is almost uniform (at −850 μV). Only at the chain end, a region of opposite polarization is detected. However, the magnetization of the chains presumably does not change sign as indicated by the uniform polarization of the d bands (see Figure 1f).

To gain more detailed insight into the quasiparticle excitations and to explore the possibility of Majorana zero modes at the chain ends, we use a superconducting Pb tip (Figure 3). This increases the energy resolution well beyond the Fermi−Dirac limit but shifts all spectral features by Δ_{tip}, the gap of the superconducting tip. Putative Majorana modes should thus appear at $eV = \pm\Delta_{tip}$. On Pb(110) (Figure 3a, gray), we resolve the double peak structure of the coherence peaks of the two-band superconductor Pb at $\pm(\Delta_{tip} + \Delta_{sample})$.[20] On the chains, we find a rich subgap structure, which varies along the chains (see Figure 3a and b for a chain of ≃10.3 nm). The most intense resonance resides close to the superconducting gap edge (labeled α in Figure 3b) and is well-separated from a broader band of resonances at lower energy (β in Figure 3b). The pronounced separation of α and β is observed for most, but not all of the chains investigated (see

DOI: 10.1021/acs.nanolett.7b01728
Nano Lett. XXXX, XXX, XXX−XXX

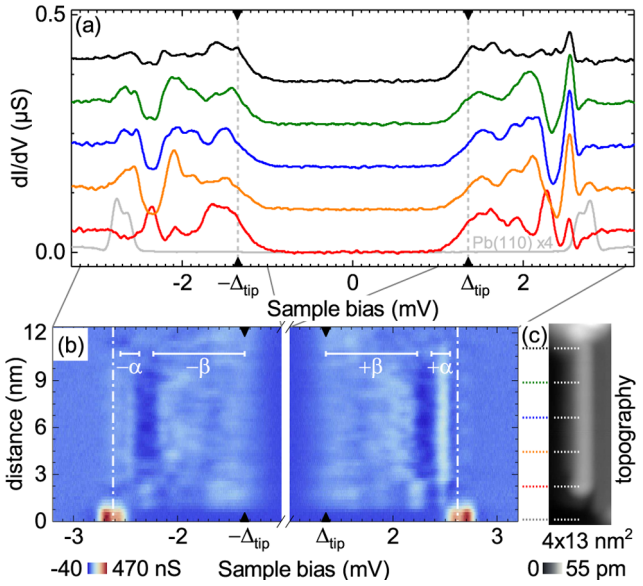

Figure 3. (a) dI/dV spectra acquired with a superconducting tip on the bare surface (gray; divided by four) and on the ≃10.3 nm long chain shown in the topography in panel c. Spectra offset by 90 nS for clarity, tip positions indicated by colored dashed lines in panel c. The tip gap is marked by dashed lines ($\pm\Delta_{tip}$ = ±1.35 meV). Set point: 5 mV, 200 pA. (b) False-color plot of all 40 dI/dV spectra measured along the central axis of the chain in panel c. Beside an intense resonance close to the gap edge [$\alpha \simeq (2.5 \pm 0.1)$ mV], spectral intensity appears mainly in the energy interval $\beta \simeq (1.8 \pm 0.4)$ mV. As a guide to the eye, the dashed−dotted lines indicate the gap edge at $eV = \pm(\Delta_{tip} + \Delta_{sample})$. See Figures S6 and S7 of the SI for additional data on this chain.

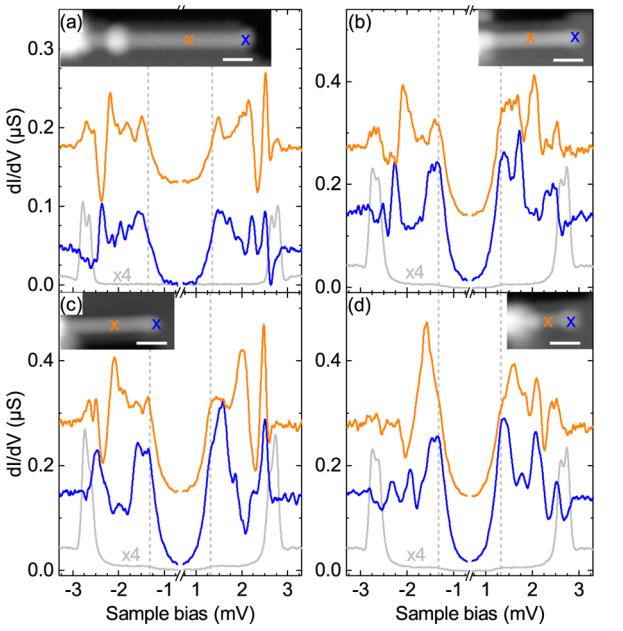

Figure 4. dI/dV spectra acquired at the end and center, respectively, of four chains with length ranging from 2.5 to 11.7 nm (tip positions marked in the corresponding topographies). The spectra were recorded with different tips with superconducting gaps of 1.35 meV for panel a, and of 1.32 meV for panels b−d, respectively. As guide to the eye the energy of the tip gap is marked by dashed lines. A spectrum of the bare surface is superimposed in gray for comparison and divided by four. The scale bars in the inset correspond to 2 nm. Spectra are offset by 0.13 μS for clarity. See Figures S8−S10 of the SI for more spectra of these chains.

Figure 4, as well as Figures S4 and S5 in the SI for data on additional chains).

The resonances persist throughout the chain but show local intensity variations arising from confinement effects and variations in the local potential.[12] At zero energy, i.e., at a bias voltage $\simeq \pm\Delta_{tip}$, we observe resonances (or shoulders), which might at first sight be reminiscent of Majorana states. However, the zero-energy signal is present all along the chain with no sign of localization at the chain end, in contrast to the expected signature for Majorana zero modes.

Next, we explore the influence of the chain length on the excitation spectrum in Figure 4 (data on additional chains with different lengths are shown in the SI). For all chains, dI/dV spectra acquired at the end exhibit a rich subgap structure and a sizable spectral intensity at $\simeq \pm\Delta_{tip}$. However, a similar spectral intensity is also present in spectra recorded in the center of the chains (in agreement with the chain presented above). We investigated 23 chains with lengths ranging from 2.5 to 11.7 nm. None of them showed a localization of zero-energy resonances at the chain end. One might argue that the distance between the end states is within the Majorana localization length. The states would then hybridize and lose their Majorana character. The splitting should be more pronounced the stronger the overlap, that is, the shorter the chain. However, we do not observe any length dependence. Furthermore, the localization length of Majorana states is expected to be on the order of atomic distances.[21] The absence of localization in any of the chains suggests that the zero-energy features cannot be assigned to a Majorana mode.

These experimental results indicate the absence of Majorana states although crucial ingredients for topological superconductivity and Majorana zero modes are fulfilled in our system: a ferromagnetic chain with spin-polarized bands at the Fermi level is coupled to an s-wave superconductor with strong spin−orbit coupling.

For a theoretical interpretation, we model the band structure of the linear Co chain. Following calculations for Fe chains,[5] we employ bulk tight-binding parameters within a Slater−Koster tight-binding approximation for the chain. Moreover, we estimate the filling of the d bands based on the number of d electrons in individual atoms. The s bands are higher in energy and thus have no significant overlap with the d bands. Because of the tendency to form a 2+ or 3+ oxidation state, hybridization with the Pb bulk bands might empty the Co s orbitals (for a more extensive discussion, see the SI). First neglecting spin−orbit coupling (Figure 5a), two broad minority bands cross the Fermi energy E_F, one of which is 2-fold degenerate. In addition, a narrow, doubly degenerate band originating from the d_{xy,x^2-y^2} orbitals lies close to the Fermi level. This band might give rise to the resonance at −0.17 mV which we observe in the dI/dV spectra on the Co chains. When including spin−orbit coupling, all d band degeneracies are lifted. Depending on the relative direction of magnetization and chain, the bands are mixed and shift in energy. We find that, unless the magnetization is perpendicular to the chain direction (Figure 5b), the system has an even number of Fermi points within half the Brillouin zone. Thus, even if most prerequisites for the formation of Majorana modes are fulfilled, the hybridization between these Fermi points would prevent the formation of a topological phase. In the case of the Fe chain,

DOI: 10.1021/acs.nanolett.7b01728
Nano Lett. XXXX, XXX, XXX−XXX

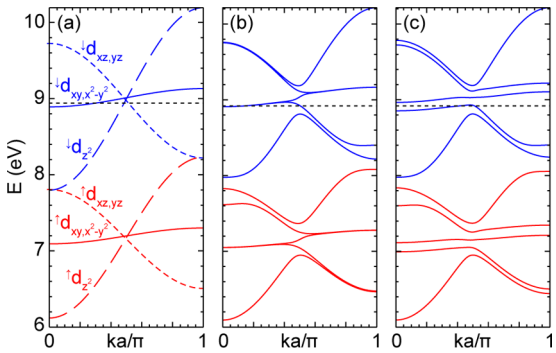

Figure 5. Tight-binding band structures of a linear Co chain with interatomic distance a = 2.486 Å and without coupling to the Pb substrate. Panels a and b,c show results without and with spin−orbit coupling, respectively. The spin−orbit coupling parameter is λ_{so} = 0.2 eV. In panel b, the adatom magnetization is perpendicular to the chain direction. In panel c, the angle between magnetization and chain direction is taken as $2\pi/5$. The exchange interaction splits minority (blue) and majority (red) bands. The black dotted lines indicate the chemical potential, which implies five Fermi points within half the Brillouin zone for panel a, three points for panel b, and two points for panel c, respectively.

the adatoms have one less d electron, resulting in a correspondingly lower E_F. In this case, there are three Fermi points, which would allow Majorana modes. We note, however, that the number of Fermi points is more robust against changes in E_F for Fe than for Co.

We finally comment on our observation of spectral weight in dI/dV at zero energy. This might be a consequence of the subgap band structure. It is possible that the induced gap is below the experimental energy resolution of ≈60 μV, the coherence peaks associated with the gap edges would then not be fully resolved and instead show as spectral weight at zero energy. Clearly, the coherence peaks are a bulk feature of the chain and the corresponding peaks in dI/dV should persist along the entire chain.

In conclusion, motivated by the predictions of topological superconductivity as a near universal feature in ferromagnetic chains on superconducting Pb, we deposited Co on Pb(110). Similar to Fe,[5,11,12] Co forms one-dimensional chains with ferromagnetic order as evidenced by a homogeneous spin polarization of the d bands. Furthermore, we resolved the spin-polarized nature of YSR bands with the perspective to probe the polarization of possible Majorana states[22,23] in experiments at lower temperatures. We observed zero-energy spectral weight along the entire chains, albeit without a clear signature of localization at the chain ends, suggesting the absence of topological superconductivity. A simple model of the one-dimensional band structure of the transition metal chains predicts an even number of Fermi points for Co, but a robust topological phase for Fe chains. This highlights the importance of the proper adjustment of the chemical potential to obtain a topologically nontrivial phase. Our work shows that it is rewarding to explore different adatom species as well as superconducting substrates to gain a deeper understanding of topological superconductivity in adatom chains.

■ ASSOCIATED CONTENT

Supporting Information

The Supporting Information is available free of charge on the ACS Publications website at DOI: 10.1021/acs.nanolett.7b01728.

A description of the experimental tip preparation of spin-polarized and superconducting tips. dI/dV spectra along the chains and dI/dV maps of the chains at different energies with a spin-polarized tip. Data of chains without a cluster at either end. Data of chains with a cluster at each end. A full set of spectra along the chains for all chains displayed in the main text. Details of the tight-binding calculations. An alternative discussion of the band filling of cobalt chains on Pb(110) (PDF)

■ AUTHOR INFORMATION

Corresponding Author

*E-mail: bheinrich@physik.fu-berlin.de. Phone: +49 (0)30 838 52 807.

ORCID

Benjamin W. Heinrich: 0000-0002-1989-6981

Notes

The authors declare no competing financial interest.

■ ACKNOWLEDGMENTS

We gratefully acknowledge funding by the Deutsche Forschungsgemeinschaft through Collaborative Research Centers Sfb 658 and CRC 183, and through Grants FR2726/4 and HE7368/2, as well as funding by the European Research Council through Consolidator Grant NanoSpin. We thank M. Font Gual and L.-M. Rütten for assistance.

■ REFERENCES

(1) Alicea, J. *Rep. Prog. Phys.* **2012**, *75*, 076501.
(2) Beenakker, C. W. *Annu. Rev. Condens. Matter Phys.* **2013**, *4*, 113−136.
(3) Elliott, S. R.; Franz, M. *Rev. Mod. Phys.* **2015**, *87*, 137−163.
(4) Mourik, V.; Zuo, K.; Frolov, S. M.; Plissard, S. R.; Bakkers, E. P. A. M.; Kouwenhoven, L. P. *Science* **2012**, *336*, 1003−1007.
(5) Nadj-Perge, S.; Drozdov, I. K.; Li, J.; Chen, H.; Jeon, S.; Seo, J.; MacDonald, A. H.; Bernevig, B. A.; Yazdani, A. *Science* **2014**, *346*, 602−607.
(6) Albrecht, S. M.; Higginbotham, A. P.; Madsen, M.; Kuemmeth, F.; Jespersen, T. S.; Nygård, J.; Krogstrup, P.; Marcus, C. M. *Nature* **2016**, *531*, 206−209.
(7) Lv, Y.-F.; Wang, W.-L.; Zhang, Y.-M.; Ding, H.; Li, W.; Wang, L.; He, K.; Song, C.-L.; Ma, X.-C.; Xue, Q.-K. *Sci. Bull.* **2017**, in press DOI: 10.1016/j.scib.2017.05.008.
(8) Ménard, G. C.; Guissart, S.; Brun, C.; Trif, M.; Debontridder, F.; Leriche, R. T.; Demaille, D.; Roditchev, D.; Simon, P.; Cren, T. *arXiv*:1607.06353, **2016**.
(9) Kitaev, A. Y. *Phys.-Usp.* **2001**, *44*, 131.
(10) Li, J.; Chen, H.; Drozdov, I. K.; Yazdani, A.; Bernevig, B. A.; MacDonald, A. H. *Phys. Rev. B: Condens. Matter Mater. Phys.* **2014**, *90*, 235433.
(11) Pawlak, R.; Kisiel, M.; Klinovaja, J.; Meier, T.; Kawai, S.; Glatzel, T.; Loss, D.; Meyer, E. *Npj Quantum Information* **2016**, *2*, 16035.
(12) Ruby, M.; Pientka, F.; Peng, Y.; von Oppen, F.; Heinrich, B. W.; Franke, K. J. *Phys. Rev. Lett.* **2015**, *115*, 197204.
(13) Feldman, B. E.; Randeria, M. T.; Li, J.; Jeon, S.; Xie, Y.; Wang, Z.; Drozdov, I. K.; Bernevig, A. B.; Yazdani, A. *Nat. Phys.* **2016**, *13*, 286−291.
(14) Pietzsch, O.; Kubetzka, A.; Bode, M.; Wiesendanger, R. *Phys. Rev. Lett.* **2004**, *92*, 057202.

DOI: 10.1021/acs.nanolett.7b01728
Nano Lett. XXXX, XXX, XXX−XXX

(15) Franke, K. J.; Schulze, G.; Pascual, J. I. *Science* **2011**, *332*, 940−944.
(16) Wiesendanger, R. *Rev. Mod. Phys.* **2009**, *81*, 1495−1550.
(17) Yu, L. *Acta Phys. Sin.* **1965**, *21*, 75.
(18) Shiba, H. *Prog. Theor. Phys.* **1968**, *40*, 435−451.
(19) Rusinov, A. I. *Zh. Eksp. Teor. Fiz. Red.* **1969**, *9*, 146−149.
(20) Ruby, M.; Heinrich, B. W.; Pascual, J. I.; Franke, K. J. *Phys. Rev. Lett.* **2015**, *114*, 157001.
(21) Peng, Y.; Pientka, F.; Glazman, L. I.; von Oppen, F. *Phys. Rev. Lett.* **2015**, *114*, 106801.
(22) Sticlet, D.; Bena, C.; Simon, P. *Phys. Rev. Lett.* **2012**, *108*, 096802.
(23) Björnson, K.; Pershoguba, S. S.; Balatsky, A. V.; Black-Schaffer, A. M. *Phys. Rev. B: Condens. Matter Mater. Phys.* **2015**, *92*, 214501.

DOI: 10.1021/acs.nanolett.7b01728
Nano Lett. XXXX, XXX, XXX−XXX